Appendix D
Design Example-Finite Element Method

D-1. General

a. The design example problem described in Appendix B was analyzed using the composite finite element-equivalent mass system method. The analysis was performed on a PC using the computer program ALGOR-Finite Element Analysis System.

b. Definitions of symbols and notations used in this appendix can be found in the Glossary. Refer to Appendix B where the values of several parameters used as input to the finite element program were developed.

D-2. Computer Model

The computer model is shown in Figures D-1 and D-2. The general characteristics are as follows:

a. The dam/foundation is a 2-D representation using the critical transverse cross section of the dam. The geometry of the finite element mesh is established by 156 node points.

b. The foundation effects are modeled using a block of foundation with the width of the block equal to 3 times the width of the dam base, and the height of the block equal to 1.5 times the height of the dam.

c. The boundary conditions along the bottom and both sides of the foundation block consist of roller restraints of the node points establishing these boundary lines.

d. Both the dam and the foundation block are modeled with 2-D solid, isotropic, quadrilateral, plane strain elements. The dam consists of 78 elements, and the foundation block consists of 48 elements. The nodes establishing the corners of the elements have 2 degrees-of-freedom (Y and Z translations).

e. The material properties for the dam RCC and the foundation block are given in Appendix B. The density of the foundation block is set to zero so the ground motion is transmitted to the dam-foundation interface without modification.

f. The reservoir effects are modeled by developing an equivalent mass system which consists of adding lumped masses to the nodal points at the upstream face of the dam as shown in Figure D-1. Procedure for determining the magnitude of the added masses is given below.

D-3. Equivalent Mass System Representation of Reservoir Effects

a. This system models the hydrodynamic effects by adding mass to the finite element model. It is founded on the equations and techniques used by Chopra in developing his simplified analysis method. It is based on the fundamental mode, but since this usually contributes 85 to 90 percent of the response, it produces good results. The method accounts for the compressibility of water and the interaction of the water with the elastic structure and foundation. The equations used in deriving the equivalent mass system for finite element analysis are:

$$f_1 = \frac{\tilde{L}_1}{\tilde{M}_1} \frac{S_A}{g} (g\bar{m}) (\psi_1) \qquad \text{(D-1)}$$

where

f_1 = total lateral force per unit height acting at a certain elevation *including* the hydrodynamic contribution

$\bar{m}$ = equivalent mass system which consists of

$$\bar{m} = m_S + m_{HD} \qquad \text{(D-2)}$$

where

m_S = mass per unit height of concrete

m_{HD} = mass per unit height which must be added to account for the hydrodynamic effects

Ψ_1 = fundamental mode shape normalized so the crest of the dam has a unit deflection

$$m_{HD} = \frac{p}{\Psi_1} \qquad \text{(D-3)}$$

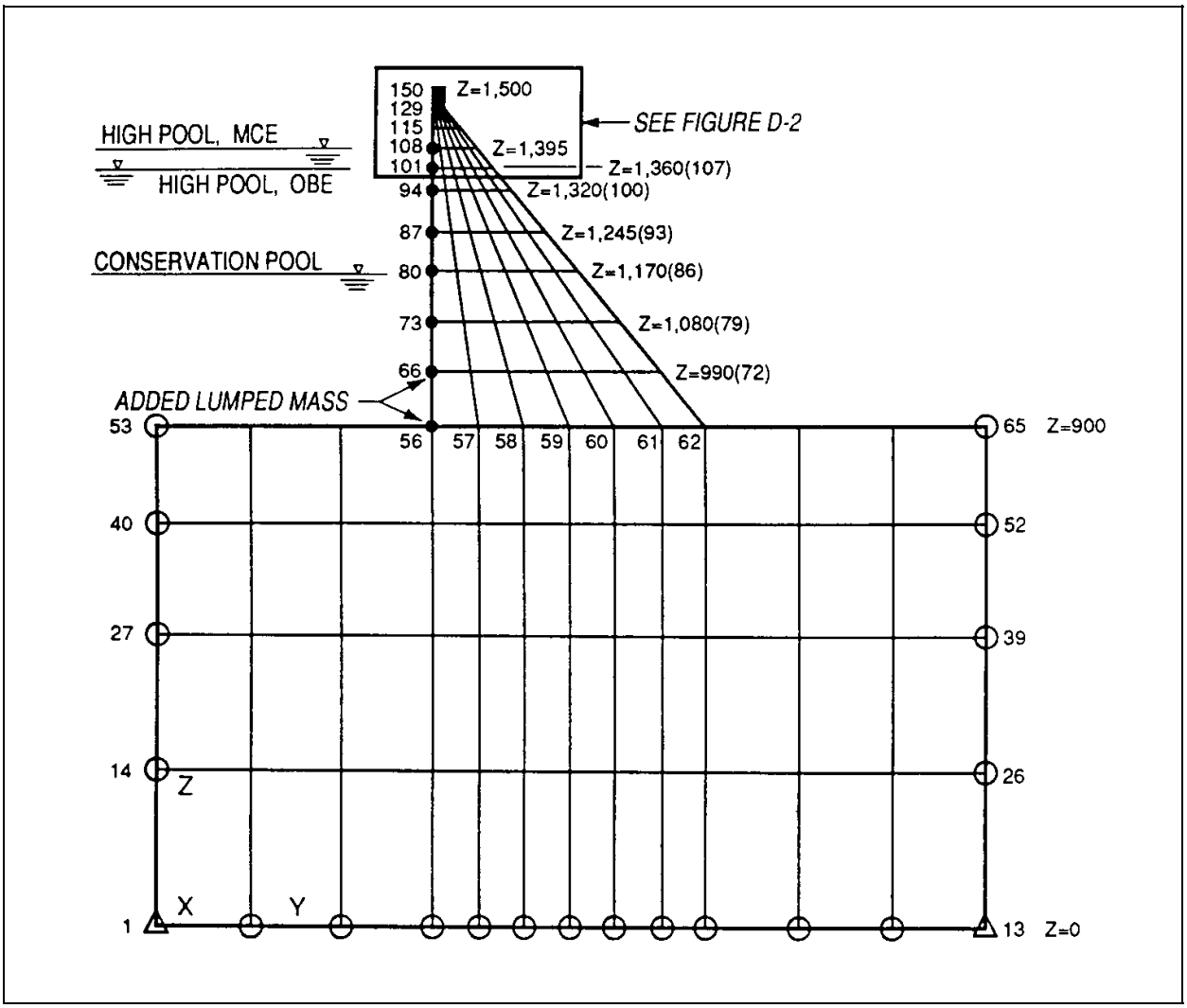

Figure D-1. Composite finite element-equivalent mass system model

where

p = the hydrodynamic pressure function determined by using Chopra's standardized curves of $\left(\frac{g\bar{p}}{wH}\right)$. This is discussed in detail later.

$$w_S = g(m_S) \qquad \text{(D-4)}$$

where

w_S = weight per unit height of concrete

b. It is now possible to substitute Equations D-2 through D-4 into Equation D-1 which gives the basic equation used in Chopra's simplified method:

$$f_1 = \frac{\tilde{L}_1}{\tilde{M}_1} \frac{S_A}{g} (w_S \Psi_1 + gp)$$

c. The above derivation shows that Chopra's simplified method is based on an "equivalent mass system." The added mass that accounts for the hydrodynamic effects is represented by m_{HD} in Equation D-3 above. This same added mass can be included in a finite element model, and it will cause the model to respond with a very good approximation of the interaction of the compressible water on the flexible structure/foundation system.

d. Chopra provides standardized curves of the hydrodynamic pressure function $\left(\frac{g\bar{p}}{wH}\right)$. It should be

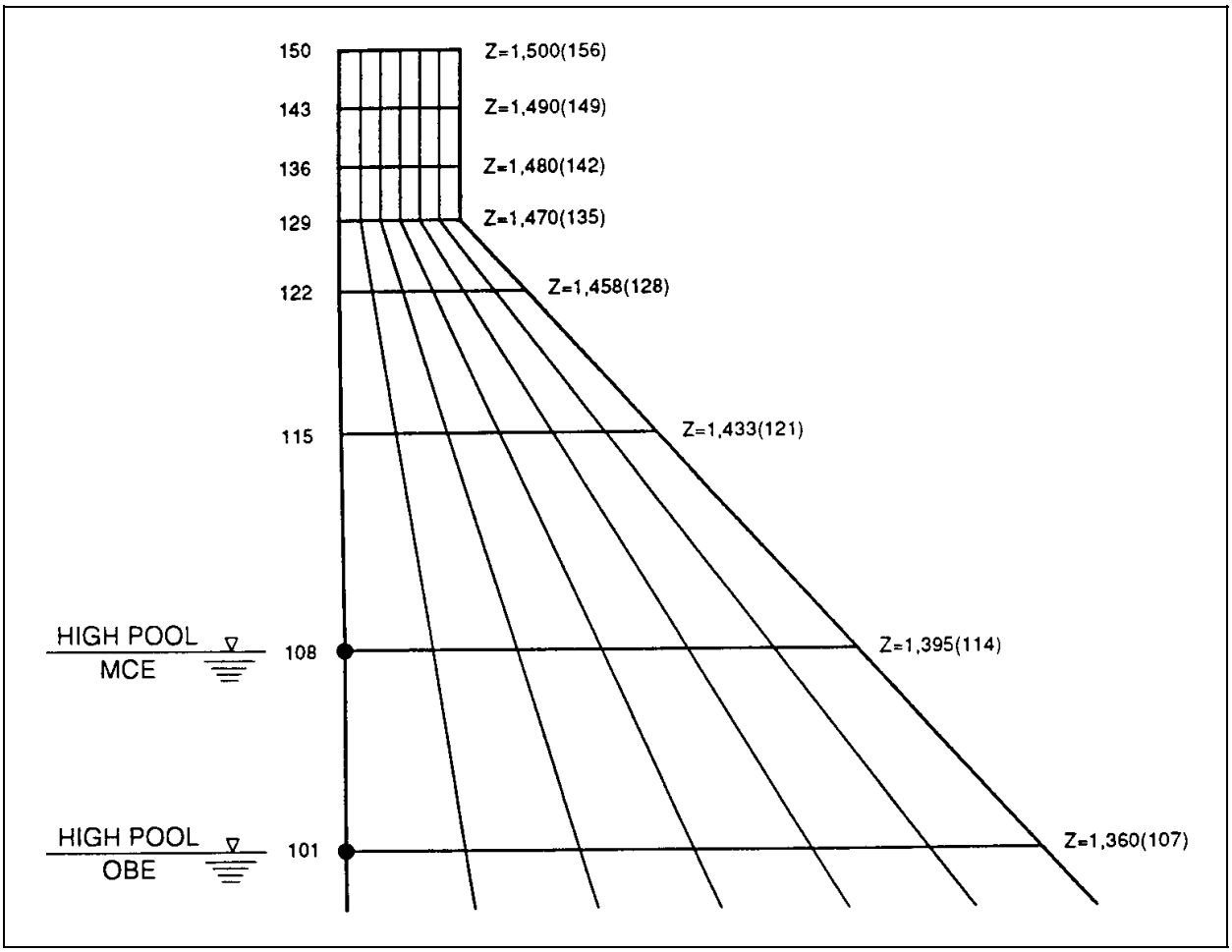

Figure D-2. Zoom-in of finite element mesh at top of dam

noted that these curves are based on the full reservoir condition where $H/H_s = 1$. To correct the values taken from the curves for other reservoir depths it is necessary to multiply these values by the following factor:

$$p = \left[\left(\frac{wH}{g} \right) \left(\frac{H}{H_S} \right)^2 \right] \left(\frac{g\bar{p}}{wH} \right)$$

where

p = hydrodynamic pressure function for a reservoir of depth H above the foundation

Then the added mass is calculated to be:

$$m_{HD} = \frac{p}{\psi_1} = \frac{1}{\psi_1} \left[\left(\frac{wH}{g} \right) \left(\frac{H}{H_S} \right)^2 \right] \left(\frac{g\bar{p}}{wH} \right) \qquad \text{(D-5)}$$

The finite element model requires the distributed mass m to be converted to lumped masses applied at appropriate nodes on the upstream face of the model as expressed by

$$M_n = C_{tr}\, m_{HD}$$

where

M_n = added lumped mass at a particular node

C_{tr} = the tributary area associated with a particular node

m_{HD} = the value of the distributed mass (mass per unit height) at a particular node location

Equation D-5 is then rewriten as:

$$M_n = \left[\left(\frac{wH}{g} \right) \left(\frac{H}{H_S} \right)^2 \right] \left(\frac{C_{tr}}{\psi_1} \right) \left(\frac{g\bar{p}}{wH} \right) \quad \text{(D-6)}$$

e. The Chopra curves for standardized pressure function are based on the ratio R_w which is defined by the following equation:

$$R_w = \frac{T_1^r}{\tilde{T}_r} \quad \text{(D-7)}$$

where

$$T_1^r = \frac{4H}{C} \quad \text{(D-8)}$$

Equations for T_r will now be derived which are based on terms that are determined by performing modal analyses using the computer model described in paragraph D-2 to extract the fundamental resonant period for the first mode and the characteristic shape of the first mode.

$$\tilde{T}_r = R_r T_1 \quad \text{(D-9)}$$

$$\tilde{T}_f = R_f T_1 \quad \text{(D-10)}$$

$$\tilde{T}_1 = R_r R_f T_1 \quad \text{(D-11)}$$

By rearranging terms of Equations D-9 and D-10, substituting into Equation D-11, and finally solving for T_r results in the following:

$$T_r = \frac{\tilde{T}_1}{\tilde{T}_f} T_1 \quad \text{(D-12)}$$

Use of these equations is further discussed in the procedure described below.

D-4. Procedure to Determine Added Lumped Masses

The following is a step-by-step procedure to determine the lumped masses to be added at the upstream node points to model the hydrodynamic effects:

Step 1. Perform the modal extraction phase of the dynamic analysis to determine the fundamental resonant period T_1 of the dam on a rigid foundation with an empty reservoir. This requires modifying the computer model described in paragraph D-2 by temporarily fixing the nodes at the dam-foundation interface to create the rigid foundation condition required for this step only. This step is referred to as *computer run #1*, and requires extracting only the first mode.

Step 2. Calculate H/H_s for the pool elevation of interest, and use Figure D-3 to determine a value of R_r. Then calculate $\tilde{T}_r$ using Equation D-9, and then calculate R_w using Equation D-7.

Step 3. With this value of R_w, use Figure D-4 to obtain values of the standard hydrodynamic pressure function ($g\bar{p}/wH$) at the locations of y/H that correspond to the upstream node point elevations. Use the R_w curve that is nearest the calculated value of R_w, but on the conservative side. Note that the appropriate value of α, the wave reflection coefficient, was calculated for the example problem in Appendix B. To determine the correct values of ($g\bar{p}/wH$) for this value of α, it will be necessary to interpolate between the appropriate pair of graphs. These values of ($g\bar{p}/wH$) are used to develop the initial added mass model (see Table D-1 for an example).

Step 4. Remove the temporary node point fixities at the dam-foundation interface leaving the computer model with the boundary conditions described in paragraph D-2, and perform the modal extraction phase of the dynamic analysis to determine the fundamental resonant period of the dam on its elastic foundation with an empty reservoir, $\tilde{T}_f$, and the corresponding characteristic mode shape for the first mode. This step is referred to as *computer run #2*, and requires extracting only the first mode.

Step 5. Normalize the first mode shape from *computer run #2* to a unit translation at the top of the dam by dividing the appropriate node point translation values by the translation value of the node at the top upstream corner of the dam. These are the values of ψ_1 for use in developing the initial added mass model.

Step 6. Using these values of ψ_1 and ($g\bar{p}/wH$), calculate the values of M_n using Equation D-6. Add

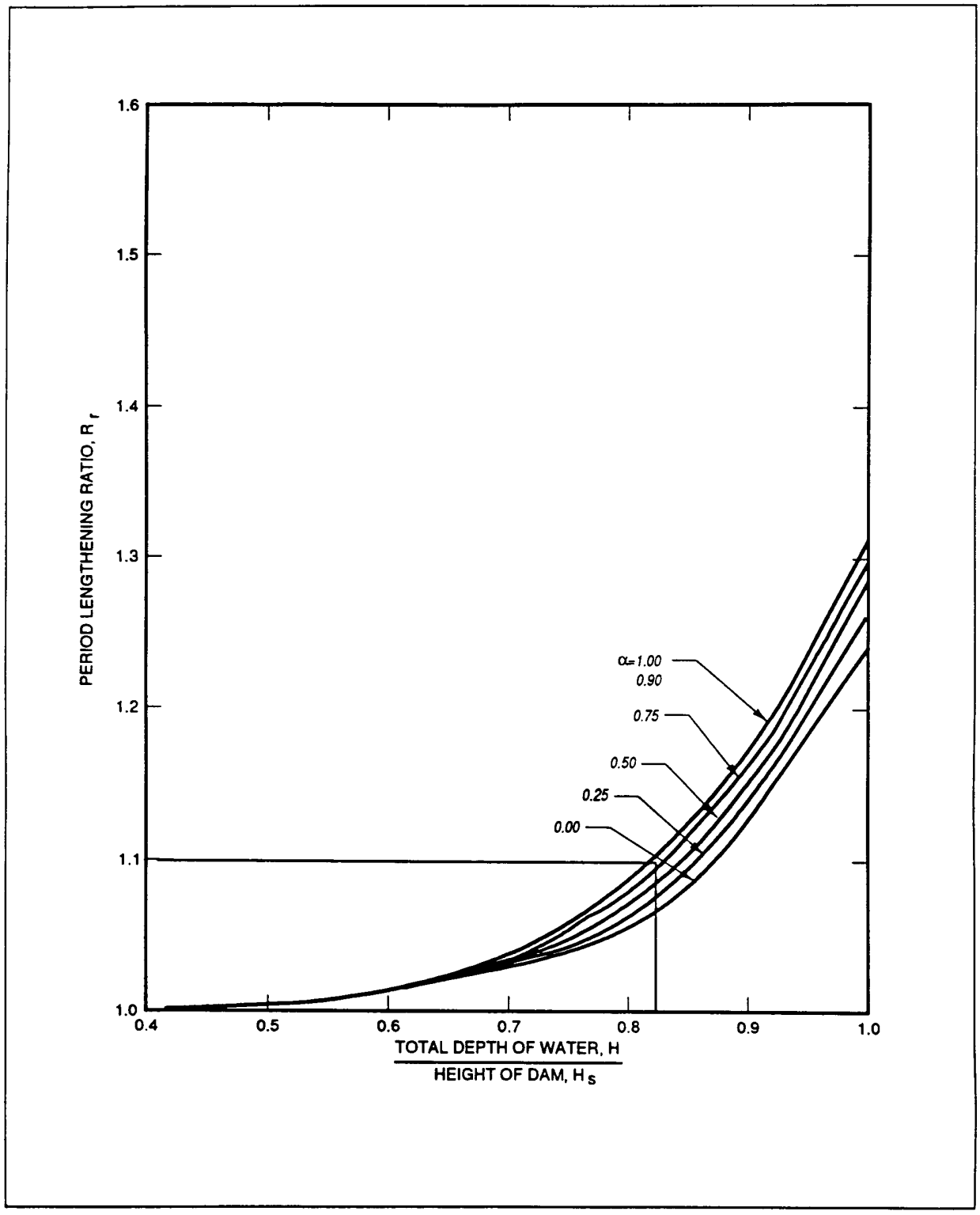

Figure D-3. Initial values of R_r, the period lengthening ratio due to hydrodynamic effects

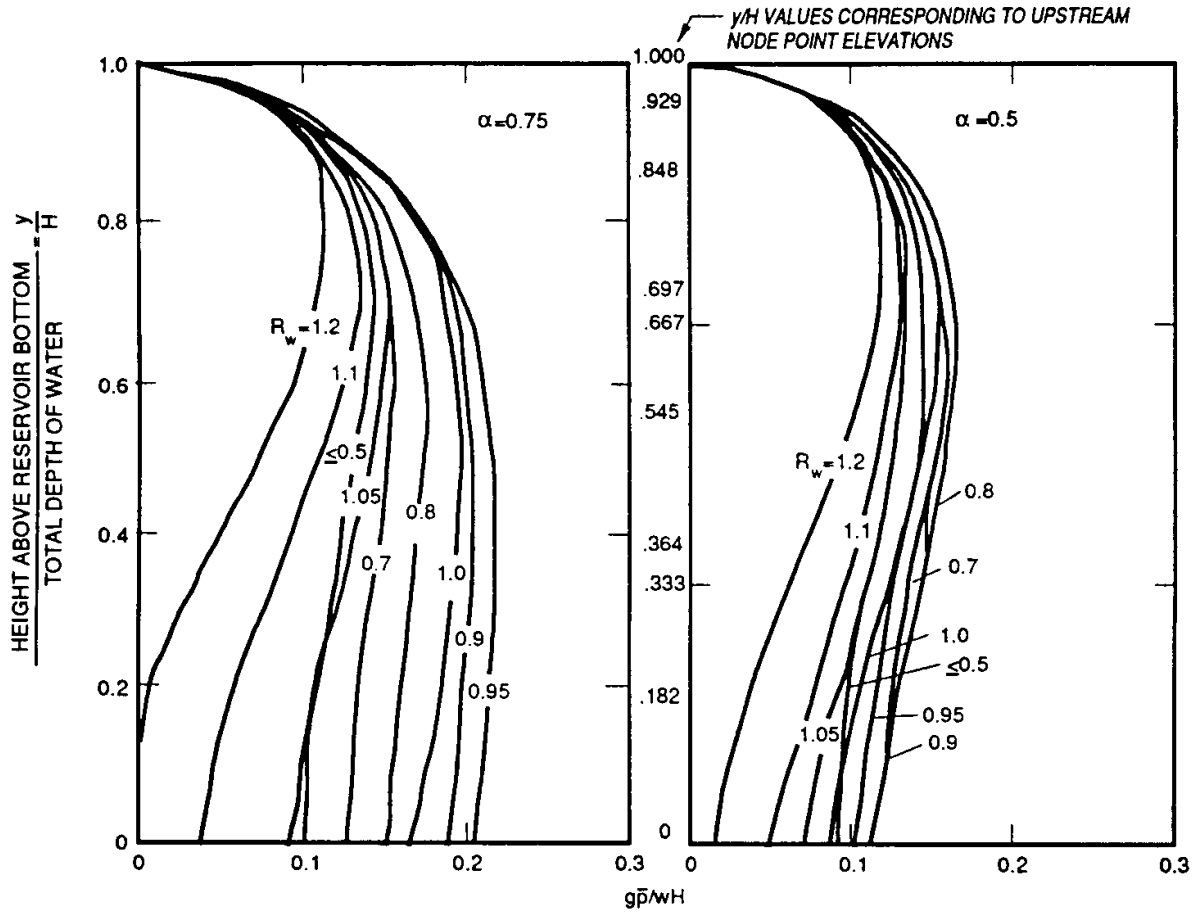

NOTE: PLOTS OF THE STANDARD VALUES FOR THE HYDRODYNAMIC PRESSURE FUNCTION $\bar{p}$; OTHER VALUES OF α ARE CONTAINED IN REPORT NO. UCB/EERC-85/10, JUNE 1986, EARTHQUAKE ENGINEERING RESEARCH CENTER, UNIVERSITY OF CALIFORNIA, BERKELEY, CALIF.

Figure D-4. Standard values for the hydrodynamic pressure function $\bar{p}$ for full reservoir, i.e. *H*/*Hs* = 1; α = 0.75 and 0.50

these lumped masses to the computer model at the appropriate upstream node points. This now becomes the initial added mass model.

Step 7. Using the initial added mass model, perform the modal extraction phase of the dynamic analysis to determine the fundamental resonant period of the dam, $\tilde{T}_1$, on its elastic foundation with reservoir of depth H, and the corresponding characteristic mode shape for the first mode. This step is referred to as *computer run #3*, and requires extracting only the first mode.

Step 8. Normalize the first mode shape from *computer run #3* to a unit translation at the top of the dam by dividing the appropriate node point translation values by the translation value of the node at the top upstream corner of the dam. These are the values of ψ_1 for use in developing the final added mass model.

Step 9. Using the values of T_1 from *computer run #1*, $\tilde{T}_f$ from *computer run #2*, and $\tilde{T}_1$ from *computer run #3*, calculate $\tilde{T}_r$ using Equation D-12. With this value of $\tilde{T}_r$, calculate R_w using Equation D-7.

Step 10. With the new value of R_w, use Figure D-4 to obtain values of the standard hydrodynamic pressure function ($g\bar{p}/wH$) at the locations of y/H that correspond to the upstream node point elevations. Use the R_w curve that is nearest the calculated value of R_w, but on the conservative side. The value of α is the same as used in step 3. To determine the correct values of ($g\bar{p}/wH$) for this value of α, it will be necessary to interpolate between the appropriate pair of graphs. These values of ($g\bar{p}/wH$) are used to develop the final added mass model (see Table D-1 for an example).

Step 11. Using the values of ψ_1 from step 8, and the values of ($g\bar{p}/wH$) from step 10, calculate the values of M_n using Equation D-6. Add these lumped masses to the computer model at the appropriate upstream node points. This completes the final equivalent mass system representation of the reservoir effects for the reservoir of depth H.

D-5. Applying Added Lumped Mass Procedure to the Example Problem

The added lumped mass procedure described in paragraphs D-3 and D-4 will be applied to the example problem. The normal pool condition associated with the MCE will be used to demonstrate the procedure. Determining the added lumped masses for the normal pool condition associated with the OBE and for low pool conditions is similar. The computer model as described in paragraph D-2 is used in the modal analyses mentioned below.

a. Initial added mass model.

H = 2445 - 1950 = 495 ft

T_1^r = 4H/C = 4(495)/4720 = 0.4195 sec (D-8)

H_s = 2550 - 1950 = 600 ft

H/H_s = 495/600 = 0.825

T_1 = 0.3882 sec from *computer run #1* where the nodes at the dam base-foundation interface (nodes 56 through 62) of the composite dam/foundation model are fixed to create the condition of a dam on a rigid foundation.

ψ_1 = the eigenvector (mode shape) for mode 1 from *computer run #2* which uses the composite dam/foundation model with empty reservoir. The lateral mode shape translations (y-direction) are taken from the mode shape computer analysis output at the upstream face node points shown in Figures D-1 and D-2, and are normalized to a unit translation at the top of the dam (by dividing each translation value by the translation output value for the node at the top upstream corner). The normalized values are entered in the appropriate column of Table D-1 for the initial added mass model.

R_r = 1.10 from Figure D-3 (for H/H_s = 0.825), which now allows the following to be calculated:

$$\tilde{T}_r = R_r T_1 = 1.10\ (0.3882) = 0.4270 \text{ sec} \quad \text{(D-9)}$$

$$R_w = T_1^r / \tilde{T}_r = 0.4195/0.4270 = 0.982 \quad \text{(D-10)}$$

($g\bar{p}/wH$) values are obtained from Figure D-4 for the values of y/H that correspond to the upstream node point elevations shown in Figure D-1. The curve lines for R_w = 0.95 are used since they are nearest

Table D-1
Computation Sheet to Determine the Added Lumped Masses to Model the Hydrodynamic Effects of the Reservoir for the Example Problem

Node No.	Normal Pool MCE H = 495 ft: Vertical Coordinate of Node	y	Element Height	C_w	$\frac{y}{H}$	Initial Added Mass Model (R_w = 0.982): Ψ_1	$\left(\frac{g\bar{p}}{wH}\right)$	M_n	Final Added Mass Model (R_w = 0.994): Ψ_1	$\left(\frac{g\bar{p}}{wH}\right)$	M_n
150	1500	Top of dam				1.000			1.000		
108	1395	495	▽	17.50	1.000	0.743	0	0	0.759	0	0
101	1360	460	35	37.50	0.929	0.671	0.105	3.83	0.691	0.104	3.68
94	1320	420	40	57.50	0.848	0.595	0.153	9.66	0.618	0.148	8.99
87	1245	345	75	75.00	0.697	0.468	0.191	19.99	0.493	0.179	17.78
80	1170	270	75	82.50	0.545	0.358	0.203	30.55	0.383	0.183	25.74
73	1080	180	90	90.00	0.364	0.246	0.199	47.54	0.268	0.175	38.38
66	990	90	90	90.00	0.182	0.151	0.190	73.95	0.169	0.161	55.99
56	900	0	90	45.00	0	0.064	0.182	83.56	0.074	0.148	58.77
$M_n = 0.653\left(\frac{C_w}{\Psi_1}\right)\left(\frac{g\bar{p}}{wH}\right)$						ΣM_n = 269.08			ΣM_n = 209.33		
Node No.	Conservation Pool H = 270 ft: Vertical Coordinate of Node	y	Element Height	C_w	$\frac{y}{H}$	Initial Added Mass Model (R_w = 0.909): Ψ_1	$\left(\frac{g\bar{p}}{wH}\right)$	M_n	Final Added Mass Model (R_w = 0.930): Ψ_1	$\left(\frac{g\bar{p}}{wH}\right)$	M_n
150	1500	Top of dam									
80	1170	270	▽	45.00	1.000	0.358	0	0	0.360	0	0
73	1080	180	90	90.00	0.667	0.246	0.193	7.48	0.248	0.193	7.39
66	990	90	90	90.00	0.333	0.151	0.196	12.38	0.153	0.196	12.22
56	900	0	90	45.00	0	0.064	0.182	13.56	0.066	0.182	13.15
$M_n = 0.106\left(\frac{C_w}{\Psi_1}\right)\left(\frac{g\bar{p}}{wH}\right)$						ΣM_n = 33.42			ΣM_n = 32.76		

the calculated value of R_w = 0.982 (on the conservative side), and the plots for α = 0.5 and 0.75 are interpolated to give the values of ($g\bar{p}/wH$) for the calculated value of α = 0.69. Values of ($g\bar{p}/wH$) are entered in Table D-1 for the initial added mass model.

M_n = the lumped masses to be added to the upstream node points which are calculated using the following:

$$M_n = [(wH/g)\ (H/Hs)^2]\ (C_{tr}/\psi_1)\ (g\bar{p}/wH) \qquad \text{(D-6)}$$

where

$$(wH/g)\ (H/Hs)^2 = (0.0624 \times 495 / 32.2)\ (0.825)^2 = 0.653$$

and

$$M_n = 0.653\ (C_{tr}/\psi_1)\ (g\bar{p}/wH)$$

b. Final added mass model.

$\tilde{T}_f$ = 0.5188 sec from *computer run #2* which uses the composite dam/foundation model with empty reservoir.

$\tilde{T}_1$ = 0.5638 sec from *computer run #3* using the composite dam/foundation model with the added lumped masses at the upstream face which represent the hydrodynamic effects of the reservoir as calculated for the *Initial Added Mass Model.*

$$\tilde{T}_r = \tilde{T}_1 T_1 / \tilde{T}_f = 0.5638\ (0.3882)/0.5188 = 0.4219 \text{ sec} \qquad \text{(D-12)}$$

$$R_w = 0.4195/0.4219 = 0.994 \qquad \text{(D-7)}$$

ψ_1 = the eigenvector (mode shape) for mode-1 from *computer run #3* which uses the composite dam/foundation model with lumped masses from the initial added mass model to represent the hydrodynamic effects of the reservoir. The lateral mode shape translations (*y*-direction) are taken from the mode shape computer analysis output at the upstream face node points, and are normalized to a unit translation at the top of the dam (by dividing each translation value by the translation output value for the node at the top upstream corner).

($g\bar{p}/wH$) values are obtained from Figure D-4 for the values of y/H that correspond to the upstream node point elevations shown in Figure D-1. The curve lines for R_w = 1.0 are used since they are so close to the calculated value of R_w = 0.994, and the plots for α = 0.5 and 0.75 are interpolated to give the values of ($g\bar{p}/wH$) for the calculated value of α = 0.69.

M_n = the lumped masses to be added to the upstream node points and are calculated using the following:

$$M_n = [\ (wH/g)\ (H/Hs)^2\ ]\ (C_{tr}/\psi_1)\ (g\bar{p}/wH) \qquad \text{(D-6)}$$

where

$(wH/g)\ (H/Hs)^2 = (0.0624 \times 495/32.2)\ (0.825)^2 = 0.653$

and

$M_n = 0.653\ (C_{tr}/\psi_1)\ (g\bar{p}/wH)$

The initial lumped mass model is then modified by replacing the lumped masses that were added to the upstream nodes with these new lumped mass values thus creating the final added mass model for the MCE high pool condition.

D-6. Effective Damping Factor

Since the dam, foundation, and reservoir respond together as a system to ground motion, the damping contribution of each component must be considered when developing the effective damping factor. As with the equivalent mass system, Chopra's equations and curves for his simplified analysis method may be utilized in the finite element approach. The equation for the effective damping factor is

$$\tilde{\varepsilon}_1 = \frac{1}{R_r}\ \frac{1}{(R_f)^3}\ \varepsilon_1 + \varepsilon_r + \varepsilon_f \qquad \text{(D-13)}$$

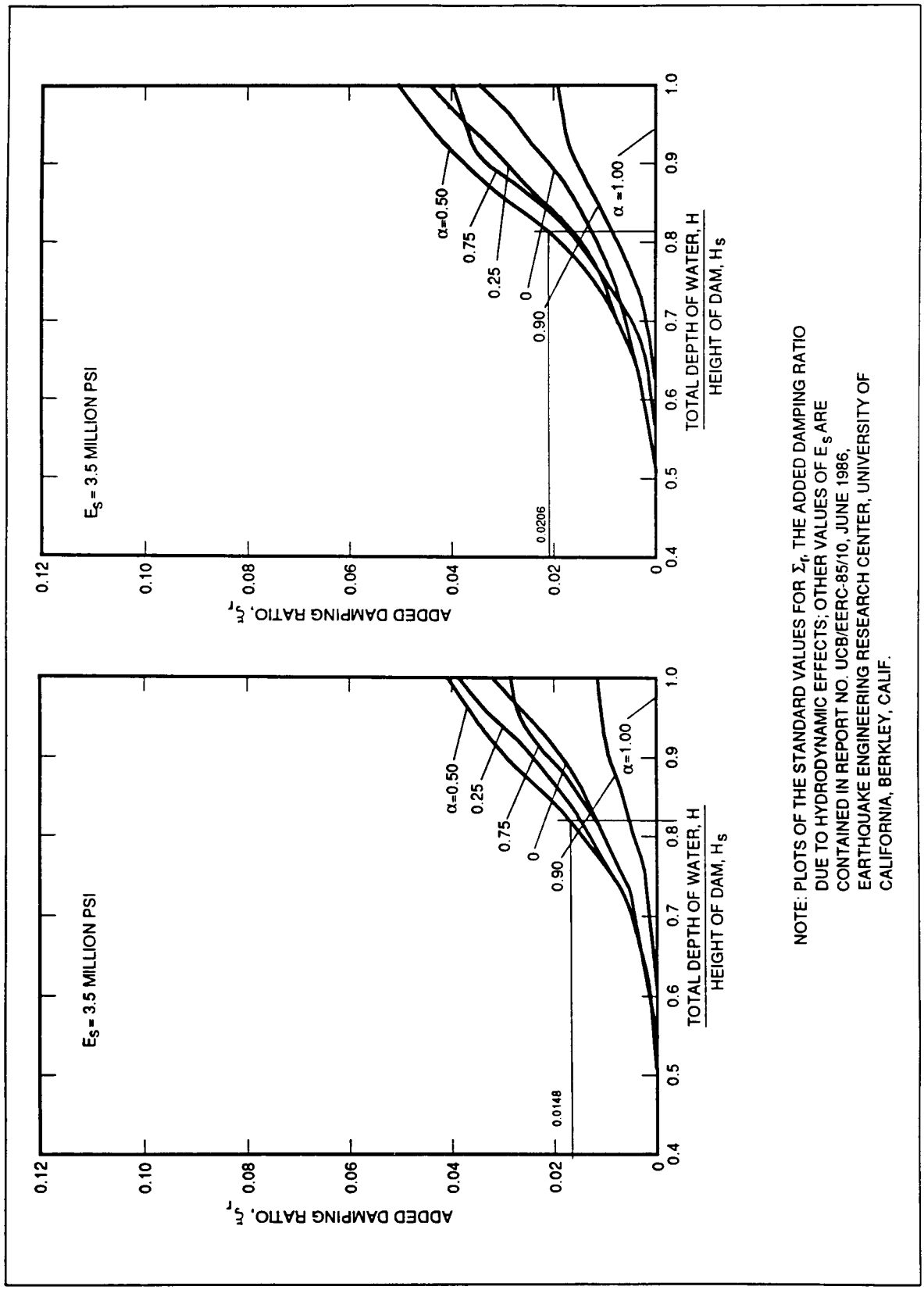

Figure D-5. Values for ε_r, the added damping ratio due to hydrodynamic effects; E_s = 3.5 and 4.0 million psi

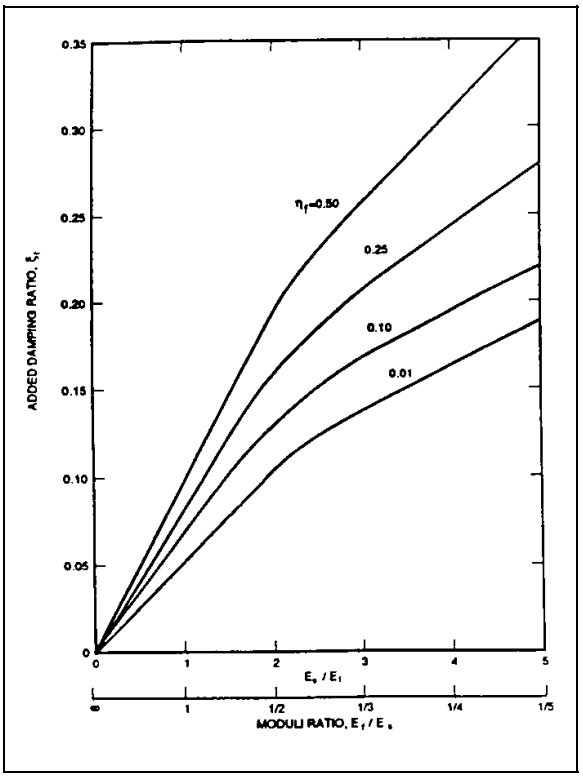

Figure D-6. Values for ε_f , the added damping ratio due to dam-foundation rock interaction

where

$\tilde{\varepsilon}_1$ = the effective damping factor

ε_1 = 5.0% for the OBE

ε_1 = 7.0% for the MCE

ε_r is taken from Figure D-5

ε_f is taken from Figure D-6

and

$$R_f = \tilde{T}_f / T_1 \qquad \text{(D-14)}$$

$$R_r = \tilde{T}_1 / T_f \qquad \text{(D-15)}$$

D-7. Procedure to Determine the Effective Damping Factor

a. Using the final added mass model, perform the modal extraction phase of the dynamic analysis to determine the fundamental resonant period of the dam, $\tilde{T}_1$, on its elastic foundation with reservoir of depth *H*. This is *computer run #4*.

b. Using the value of T_1 from *computer run #1*, $\tilde{T}_f$ from *computer run #2*, and $\tilde{T}_1$ from *computer* run #4, calculate R_f using Equation D-14, and R_r using Equation D-15.

c. Determine the value of ε_r from Figure D-5 interpolating between the appropriate curve lines for the required value of α, and between the appropriate pair of graphs for the required value of E_s. Note that the appropriate value of α, the wave reflection coefficient, and E_s, the seismic modulus of elasticity, were calculated for the example problem in Appendix B.

d. Determine the value of ε_f from Figure D-6. If the constant hysteretic damping factor for the foundation is not known, assume $n_f = 0.10$.

e. Calculate the effective damping factor using Equation D-13.

D-8. Applying Damping Factor Procedure to the Example Problem

The procedure for determining the effective damping factor will be applied to the example problem. The high pool condition associated with the MCE, and the conservation pool (low pool) condition for the MCE will be used to demonstrate the procedure.

T_1 = 0.3882 sec from *computer run #1*

$\tilde{T}_f$ = 0.5188 sec from *computer run #2*

$\tilde{T}_1$ = 0.5575 sec (normal pool for MCE) from *computer run #4*

$\tilde{T}_1$ = 0.5208 sec (low pool for MCE) from *computer run #4*

R_f = $\tilde{T}_f / T_1$ = 0.5188/0.3882 = 1.3364 (Equation D-14)

R_r = $\tilde{T}_1 / T_f$ = 0.5575/0.5188 = 1.075 (normal pool for MCE, Equation D-15)

R_r = $\tilde{T}_1 / T_f$ = 0.5208/0.5188 = 1.003 (low pool for MCE, Equation D-15)

H = 2550 - 1950 = 600 ft

H_s = 2445 - 1950 = 495 ft (normal pool for MCE), and H/H_s = 0.825

H_s = 2220 - 1950 = 270 ft (low pool for MCE), and H/H_s = 0.450

α = 0.69, E_s = 3590 ksi, and E_f = 3500 ksi as calculated in Appendix B

ε_r = 0.0158 (normal pool for MCE) from Figure D-5 for H/H_s = 0.825, interpolating between the α = 0.50 and 0.75 curve lines for the required value of α = 0.69, and also interpolating between the graphs of E_s = 3.5 million psi and 4 million psi for the required value of E_s = 3590 ksi

ε_r = 0.0 (low pool for MCE). When $H/H_s < 0.5$, ε_r = 0.0

ε_f = 0.0703 from Figure D-6 for E_s/E_f = 3590/3500 = 1.025, and an assumed value of n_f = 0.10

ε_1 = 7.0 percent

$\tilde{\varepsilon}_1$ = $(1/1.075)(1/(1.3364)^3)(7.0) + 100(0.0158) + 100(0.0703)$ = 11.34 percent (normal pool for MCE, using Equation D-13)

$\tilde{\varepsilon}_1$ = $(1/1.003)(1/(1.3364)^3)(7.0) + 100(0.0) + 100(0.0703)$ = 9.95 percent (low pool for MCE, using Equation D-13)

D-9. Design Response Spectra

As discussed in Appendix B, the conditions for this example problem require a site-specific design response spectra. However, since this is only for the purpose of demonstrating the finite element method, the standard design response spectra shown in Figure 5-1 and Table 5-1 will be assumed to be the site-specific design response spectra.

a. Normalized design response spectra. The design response spectra normalized to a PGA = 1.0 g is calculated as follows:

$\tilde{T}_1$ = 0.5575 sec for the MCE normal pool

$\tilde{T}_1$ = 0.5208 sec for the MCE low pool

The design response spectra needs to be defined only for values of the period T up to the above values of $\tilde{T}_1$.

β = $\tilde{\varepsilon}_1$ = 11.34% normal pool for MCE

β = $\tilde{\varepsilon}_1$ = 9.95% low pool for MCE

K_2 = 1.466 - 0.2895ln(11.34) = 0.76300 normal pool for MCE

K_2 = 1.466 - 0.2895**ln**(9.95) = 0.80085 low pool for MCE

K_3 = log(2.5 × 0.76300) = 0.28046 normal pool for MCE

K_3 = log(2.5 × 0.80085) = 0.30149 low pool for MCE

S_a = spectral acceleration for period = T

S_a = $10.0^{K_1 K_3}$ for $T < 0.400$

S_a = $K_2 S_{a(5\%)}$ for $T > 0.400$

b. Scaling factors-horizontal component of ground motion. The above normalized design spectra are scaled according to the scaling factors in Table 5-2. The site is located in seismic Zone 3; therefore, the scaling factors for the horizontal component of ground motion = PGA = the following:

OBE: 0.210 g

MCE: 0.550 g

c. Design response spectra for the vertical component of ground motion. In accordance with the requirements of paragraph 5-6, independent vertical component site-specific design response spectra are required for the example problem. However, for demonstration purposes, the standard design response spectra normalized to a PGA = 1.0 g as described above will be assumed to also be the vertical component site-specific design response spectra. The scaling factors for the vertical component of ground motion will be based on Figure 5-3 as follows:

T = period (sec)	$S_{a(5\%)}$ (g's)	K_1	S_a MCE Normal Pool (g's)	S_a MCE Low Pool (g's)
0.002	1.0000	0.00000	1.0000	1.0000
0.010	1.0000	0.00000	1.0000	1.0000
0.020	1.2643	0.25596	1.1797	1.1945
0.040	1.5985	0.51192	1.3918	1.4267
0.060	1.8335	0.66164	1.5331	1.5830
0.080	2.0210	0.76787	1.6419	1.7041
0.100	2.1795	0.85028	1.7317	1.8045
0.120	2.3182	0.97160	1.8728	1.9630
0.150	2.5000	1.00000	1.9075	2.0021
0.400	2.5000	1.00000	1.9075	2.0021
0.450	2.2222		1.6955	1.7796
0.500	2.0000		1.5260	1.6017
0.550	1.8182		1.3873	1.4561
0.600	1.6667		1.2717	1.3348

R = source to site distance = 35 km (see Appendix B)

$\tilde{T}_1$ = 0.5577 sec for the MCE normal pool

$\tilde{T}_1$ = 0.5208 sec for the MCE low pool

Based on these data, the ratio of (PGA of vertical component)/(PGA of horizontal component) = 0.5. Therefore, the scaling factors for the vertical component of ground motion are

OBE = 0.5 × 0.210 = 0.105 g

MCE = 0.5 × 0.550 = 0.275 g

D-10. Response to Ground Motion

The procedure has now progressed to the point where it is possible to determine the dynamic response to the ground motion associated with the design earthquakes (the OBE and the MCE). For demonstration purposes the example problem is considering only the MCE; however, determining the response for the OBE would follow the same procedure. A summary of the work steps completed thus far is as follows:

Step 1. The computer model of the dam/foundation system has been formulated.

Step 2. Two critical earthquake load cases for the MCE have been identified, one combining the design earthquake with the normal pool condition which is considered reasonable at the time of the MCE event, and the second load case combining the design earthquake with the lowest possible pool at the time of the MCE event (the conservation pool).

Step 3. The hydrodynamic effects of these two pool elevations have been determined in terms of added lumped mass attached to the upstream face at appropriate node points. Thus the single computer model of step 1 becomes two added mass computer models, one for the normal pool load case and one for the low pool case.

Step 4. The effective damping factors for the combined dam/foundation/reservoir system have been determined for both the normal pool and low pool load cases.

Step 5. The design response spectra have been developed for the two effective damping factors.

a. Modal analysis.

(1) The next step in the procedure is to perform the final, complete modal analysis. This computer run will extract all the modes which will make a

significant contribution to the response. This requires some judgment, but 10 modes normally suffice for the typical gravity dam cross section like that of the example problem. Therefore, the first 10 modes will be extracted and the modal participation factors for these 10 modes will be examined to ensure adequate precision in the response spectrum analysis to follow.

(2) The modal participation factors are a function of the mode shape and the mass distribution. They are not influenced at all by ground motion as expressed by the response spectrum. They only give an indication of the energy absorbing capability of a particular mode. Along with the participation factors, the response spectrum also has an obvious effect on the response (deflection, stress .... etc.). Thus, the contribution for a given mode is not directly proportional to the participation factor. However, the participation factor can be used for the purpose of judging a reasonable cutoff point where higher modes would not contribute significantly to the total response based on a reasonable precision for the analysis.

(3) The modal participation factors for the first 10 modes produced by both the added mass computer models are given in the accompanying tabulation.

(4) The tabulations of modal participation factors indicate that the fundamental mode for the horizontal (*y*-direction) component of ground motion is mode 1. It is also apparent that for the horizontal component of ground motion, mode 7 through mode 10 have participation factors no greater than 1/14th of the participation factor for mode 1. Therefore, it is judged that modes 1 through 6 would have been adequate for the analysis for the horizontal component of ground motion. The fundamental mode for the vertical (*z*-direction) component of ground motion is mode 2. For this component, mode 6 through mode 10 have participation factors no greater than 1/16th of the participation factor for mode 2. Therefore, it is judged that modes 1 through 5 would have been adequate to determine the response for the vertical component of ground motion. On this basis, it is concluded that for the example problem, the

MCE Normal Pool Load Case
1** Modal Participation Factors**

Mode	X-Direction	Y-Direction	Z-Direction	period (sec)
1	0.0000E+00	2.4886E+01	4.7916E+00	5.5753E-01
2	0.0000E+00	1.1126E+01	-2.4501E+01	2.8220E-01
3	0.0000E+00	-1.2864E+01	-1.0706E+01	2.4083E-01
4	0.0000E+00	-6.8721E+00	-2.0829E+00	1.4334E-01
5	0.0000E+00	8.3296E-01	4.3875E+00	1.0627E-01
6	0.0000E+00	3.2880E+00	-3.8116E-01	9.7209E-02
7	0.0000E+00	-1.5844E+00	1.4926E+00	8.9524E-02
8	0.0000E+00	-1.3661E+00	9.1764E-02	8.0562E-02
9	0.0000E+00	1.7230E+00	-2.4378E-02	7.6114E-02
10	0.0000E+00	-9.1725E-01	1.1421E-01	7.0581E-02

MCE Low Pool Load Case
1** Modal Participation Factors**

Mode	X-Direction	Y-Direction	Z-Direction	period (sec)
1	0.0000E+00	2.2133E+01	5.4826E+00	5.2080E-01
2	0.0000E+00	9.0977E+00	-2.5568E+01	2.7845E-01
3	0.0000E+00	1.3024E+00	7.4132E+00	2.2800E-01
4	0.0000E+00	-6.4719E+00	-2.5863E+00	1.3591E-01
5	0.0000E+00	2.8372E-01	-4.3314E+00	1.0239E-01
6	0.0000E+00	3.3446E+00	-5.1985E-01	9.1338E-02
7	0.0000E+00	-5.1590E-02	-4.2117E-01	7.9362E-02
8	0.0000E+00	-7.3791E-01	-1.9763E-01	7.1327E-02
9	0.0000E+00	-1.5412E+00	-9.8779E-01	6.4530E-02
10	0.0000E+00	9.7924E-01	-1.3636E+00	6.2772E-02

response spectrum analysis using the first 10 modes of vibration for both load cases will produce the dynamic response well within the required precision.

(5) Figure D-7 shows the results of the modal analysis in the form of the mode shapes for the first six modes which were extracted from the equivalent mass system model for the normal pool. The low pool mode shapes are similar to these.

b. Response spectrum analysis.

(1) With the significant mode shapes and frequencies extracted, the design response spectrum developed in paragraph D-9 is introduced into the dynamic analysis. For each significant mode, the modal analysis produced the normalized mode shape, the natural period or frequency, and the participation factor for each ground motion component direction. The spectral ordinate corresponding to the period or frequency of each mode is the only additional parameter required to determine the maximum response for each mode for each ground motion component direction. The procedure is simple. A mode coefficient is calculated as a function of the participation factor and the spectral ordinate, and the maximum modal response, in terms of the deflected shape, is simply the mode coefficient times the normalized mode shape. The maximum modal stresses are then computed once the displaced shape is known.

(2) For each mode and for each ground motion component direction, there is a complete set of stresses. Therefore, the example problem has 20 complete sets of maximum modal stresses for each earthquake load case. The final phase of the dynamic analysis is to combine these 20 sets of stresses into a single set of stresses representing the maximum dynamic response to the design earthquake for that earthquake load case. This phase of analysis can be subdivided into two steps as follows:

Step 1. Combine each set of 10 maximum modal stresses to produce the maximum component response for each of the two ground motion component directions.

Step 2. Combine the two maximum component responses for each of the two ground motion component directions to give the final maximum dynamic response.

(3) For the example problem, paragraph 7-7*e* requires that the maximum modal stresses (step 1 above) be combined using the complete quadratic combination (CQC) method. Unfortunately, the ALGOR Finite Element program does not provide the CQC option; however, it does provide the ten percent method (TPM) discussed in paragraph 7-7*d*. Similar to the CQC, the TPM will give additional accounting to modes with nearly the same frequencies. It is noted from the above tables, the first 5 or 6 modal frequencies are well separated, so it is unlikely that there would be significant difference in the results produced by CQC or TPM for this example problem. Therefore, each set of 10 maximum modal stresses will be combined by the TPM to produce the maximum component response for the Y-direction ground motion component and the Z-direction ground motion component.

(4) Referring to paragraph 7-8*e*, the maximum component responses are to be combined by the square root of the sum of the squares method (SRSS) to produce the final maximum dynamic response.

D-11. Results of the Response Spectra Dynamic Analyses

a. As discussed in Chapters 4 and 5 of this EP, an acceptable response to the design earthquakes is based on satisfying allowable tensile stress criteria to prevent or control the extent of concrete cracking. Two different allowable tensile stresses were established, one for the parent RCC, and a lesser allowable for the lift joints. It is also noted that there are two allowables for the OBE, and two greater allowables for the MCE.

b. Based on the acceptance criteria stated above, it is necessary to determine the maximum principal tensile stress at critical node points of the computer model to determine if the design satisfies the allowable tensile stress for the parent RCC. It should be noted that the response spectrum analysis first produces the maximum modal stresses that occur at the node points, and these stresses are broken down into their component stresses in the global coordinate system. The ALGOR computer program uses these component stresses for each mode to calculate the principal tensile stress for that mode (at each node

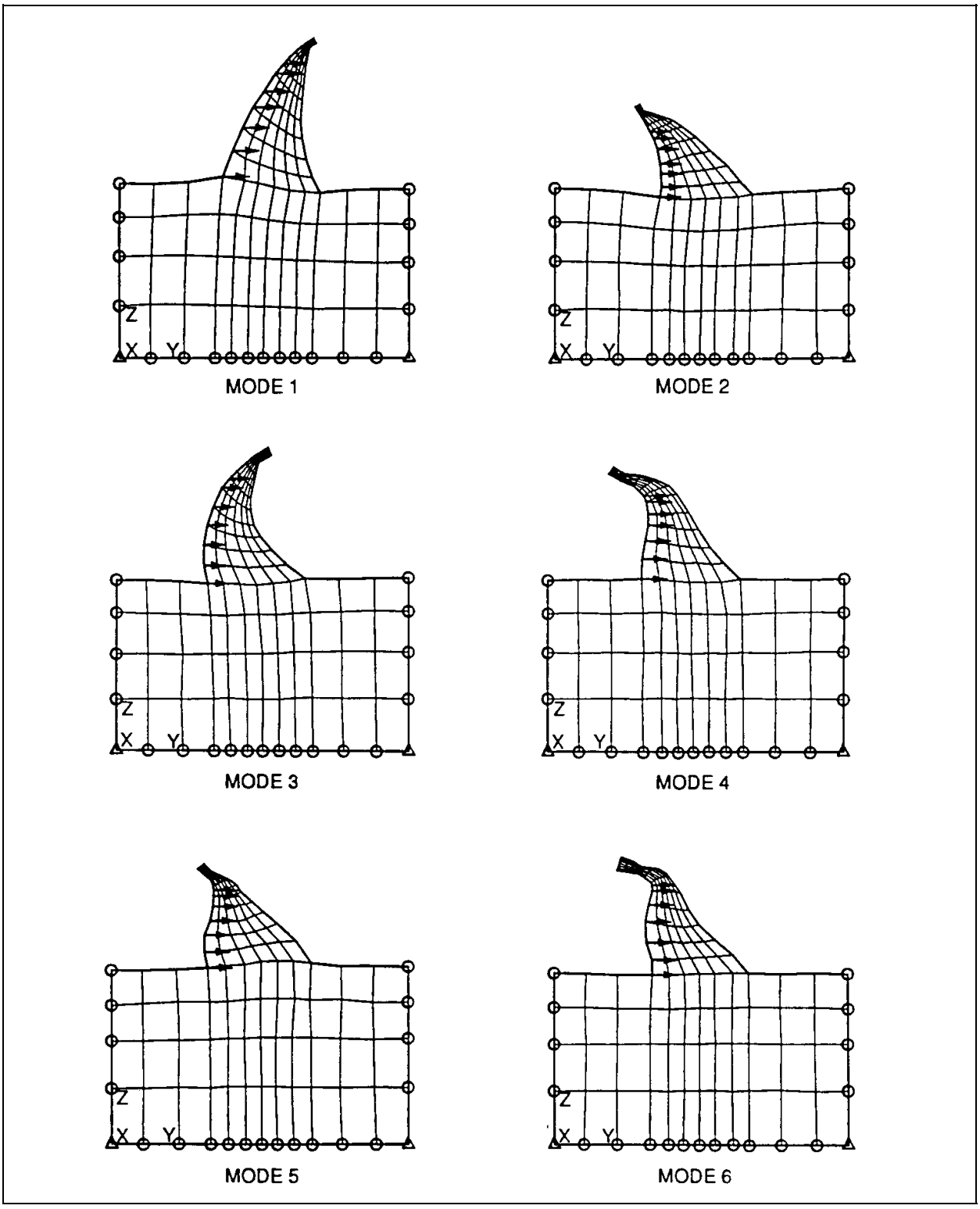

Figure D-7. Results of modal analysis-mode shapes 1 through 6 from composite finite element-equivalent mass system model for the MCE normal pool load case

point), and it then combines these individual mode principal tensile stresses by the requested modal combination method (the 10 percent method was used for the example problem) to produce the maximum principal tensile stress at each node. However, the orientation (or direction) of the principal stress vector is different for each mode, so the combined maximum principal tensile stress is not theoretically correct, but in most instances it can be considered to be a reasonably conservative estimate. In contrast to this method, other computer programs will first combine the component stresses for each mode using the requested modal combination method, and then calculate the principal tensile stress from the combined component stresses. The problem with this method is that the signs of the component stresses are lost in the combination process because all of the combination methods involve taking square roots of the sums of the squares. Again, the maximum principal tensile stress calculated from the combined (and always nonnegative) component stresses is not theoretically correct, but in most instances it produces a reasonably conservative estimate.

c. Based on the acceptance criteria stated earlier, it is also necessary to determine the maximum tensile stress normal to the plane of the horizontal lift joints to determine if the design satisfies the allowable tensile stress for the lift joints. For the computer models used in the dynamic analyses, this represents the component stress vector in the global-Z direction. It is noted that the problems associated with the principal tensile stress calculation are not inherent in combining the Z-direction component stress vectors for each of the modes using the required modal combination method. Thus, the combined Z-direction component stress vector at each node point correctly represents the maximum tensile stress normal to the lift joint at that node.

d. The maximum principal tensile stresses occur near the upstream and downstream faces of the dam in much the same manner as the maximum stresses in a beam in flexure occur at the extreme fibers of the cross section. It is also noted that the direction of the maximum principal tensile stresses near the upstream and downstream faces, for a typical dam cross section, is approximately parallel to the upstream and downstream faces, respectively. Therefore, the difference between the maximum principal tensile stress at the typically near vertical upstream face and the maximum tensile stress normal to the lift joints at the upstream face is small. Thus, the stresses normal to the lift joints will govern along the upstream face since the allowable tensile stress normal to the lift joints is considerably less than the allowable tensile stress for the parent concrete. Figure D-8 presents graphically the stress contours of the maximum tensile stresses normal to the lift joints for both MCE load cases. It is noted that these results represent only the dynamic response to the ground motion shaking. Static stresses such as the dead load weight of the dam or the hydrostatic load acting against the upstream face are not included in these results.

e. Since the direction of the maximum principal tensile stresses near the sloping downstream face is approximately parallel to the face, it is more difficult to predict whether the tensile stresses normal to the lift joints or the principal tensile stresses in the parent concrete will be critical. Therefore, both sets of stresses must be determined along the downstream face. Figure D-9 shows graphically the stress contours of the maximum principal tensile stresses that will occur near the downstream face of the dam for both MCE load cases. Note that these maximum principal tensile stresses occur during that part of the oscillation cycle when the top of the dam is translating upstream. It is noted that these results represent only the dynamic response to the ground motion shaking. Static stresses such as the dead load weight of the dam or the hydrostatic load acting against the upstream face are not included in these results.

D-12. Static Analyses

a. To complete the dynamic analyses for each earthquake load case, it is necessary to determine the static state condition of the RCC dam at the time of the design earthquake event. For the design example the static loads acting on the dam at the time of the earthquake are:

(1) Dead load weight of the RCC.

(2) Hydrostatic pressure of the reservoir against the upstream face of the dam.

b. By activating the minus Z-direction gravitational element load option in the ALGOR computer program, the dead weight of the elements is internally computed and distributed to the element corner node points. The hydrostatic loading was calculated as concentrated Y-direction forces acting on the

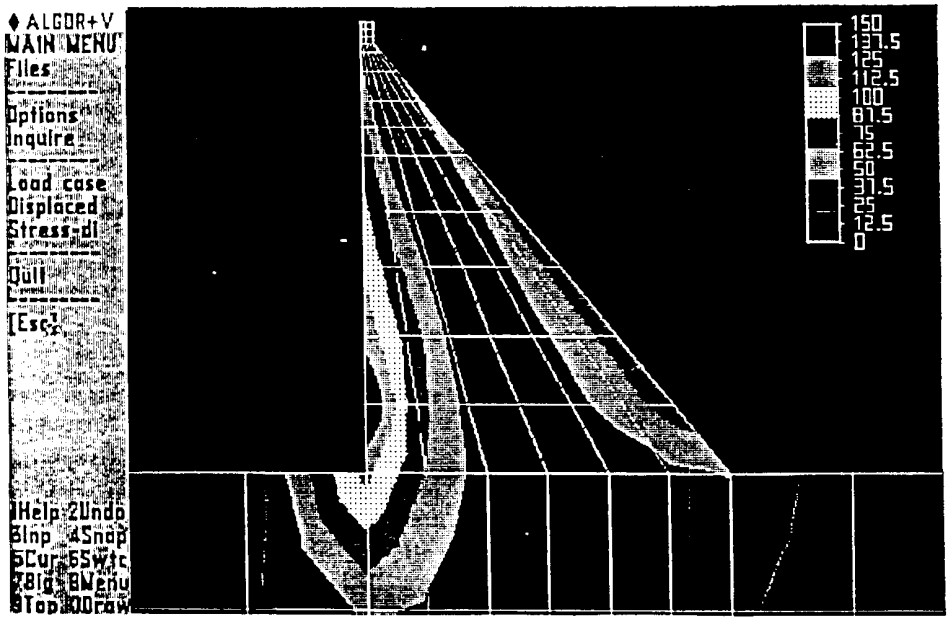

Maximum Tensile Stress Normal to Lift Joints (KSF) - MCE Normal Pool Load Case - for Full Oscillation Cycle

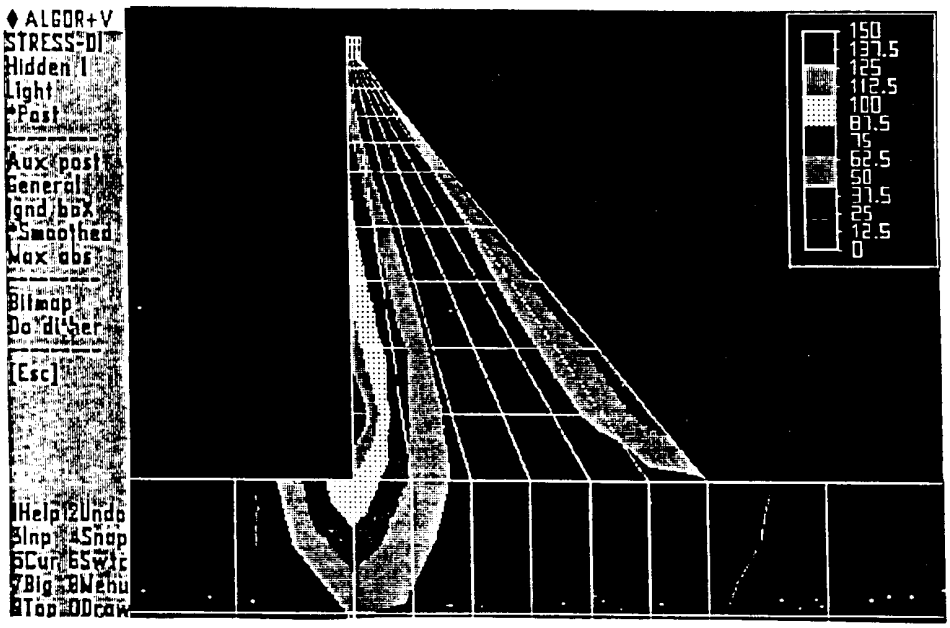

Maximum Tensile Stress Normal to Lift Joints (KSF) - MCE Low Pool Load Case - for Full Oscillation Cycle

Figure D-8. Results of response spectrum analysis-dynamic response to combined horizontal and vertical components of ground motion for MCE load cases--expressed as maximum tensile stresses normal to the lift joints

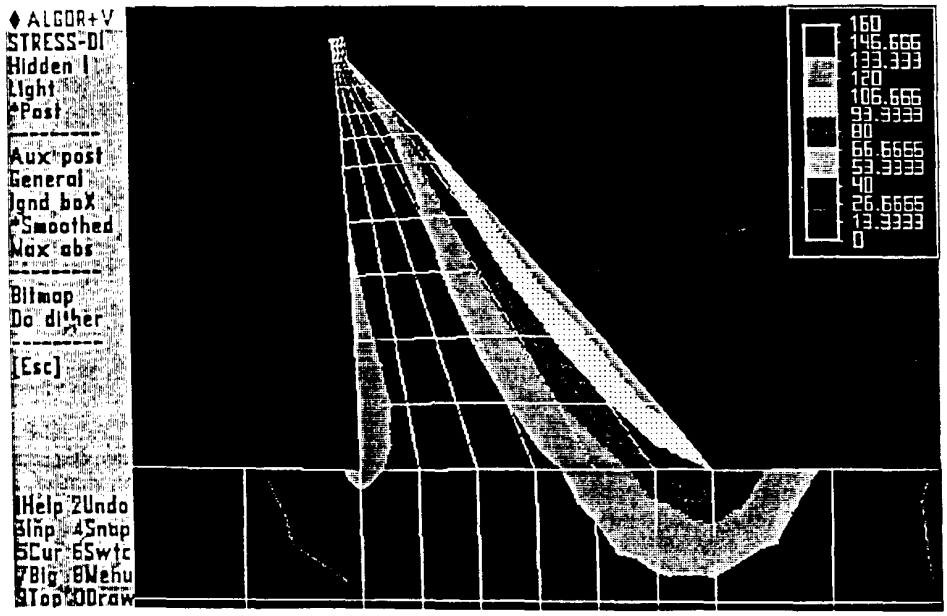

Maximum Principal Tensile Stress (KSF) - MCE Normal Pool Load Case for Upstream Translation Part of Oscillation Cycle Only

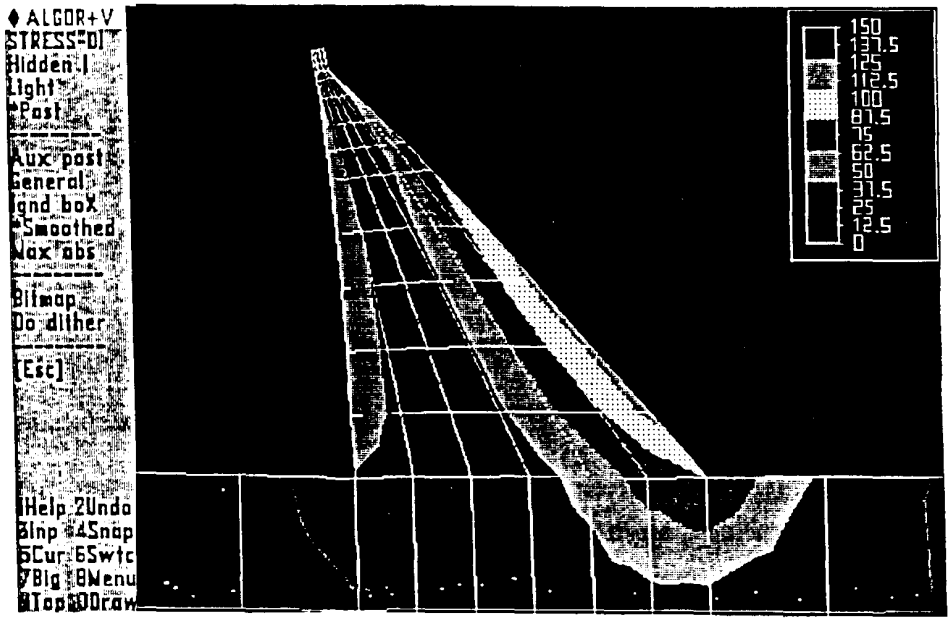

Maximum Principal Tensile Stress (KSF) - MCE Low Pool Load Case for Upstream Translation Part of Oscillation Cycle Only

Figure D-9. Results of response spectrum analysis-dynamic response to combined horizontal and vertical components of ground motion for MCE load cases--expressed as maximum principal tensile stresses.

appropriate upstream face node points. Figure D-10 shows the calculations for the hydrostatic load.

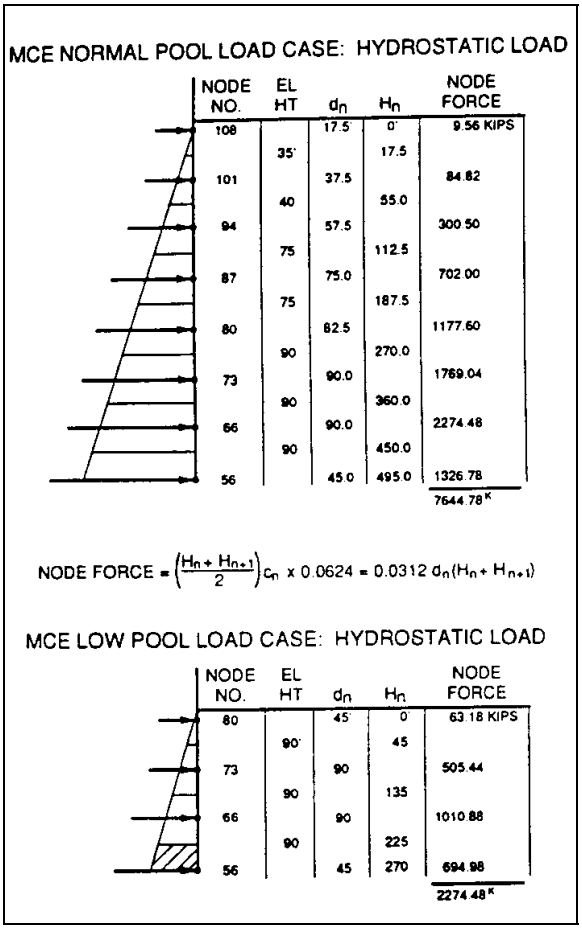

Figure D-10. Computation sheet to determine the forces to apply to the upstream node points to represent the hydrostatic pressure of the pool

c. With these loads applied to the computer model, a static finite element analysis was executed to determine the static stresses. The static stresses normal to the lift joints for both the high pool and low pool conditions are shown graphically in Figure D-11, and the principal static stresses are shown in Figure D-12.

D-13. Allowable Tensile Stress

Appendix B established the direct tensile strength of the basic RCC mix to be:

f'_t = 290 psi (for the parent concrete)

f'_t = 205 psi (for the lift joints)

Because of the high strain rates associated with a seismic event, the dynamic tensile strength is greater than the direct tensile strength obtained from the lab tests:

DTS = 1.5 f'_t = 1.5 x 290 = 435 psi (for the parent concrete)

DTS = 1.5 f'_t = 1.5 x 205 = 307 psi (for the lift joints)

In accordance with paragraph 4-2*c*, the allowable tensile stress for a new RCC dam in seismic zone 3 for the OBE load condition is:

$f_{t(allowable)}$ = 0.90 × 435 = 392 psi (for the parent concrete)

$f_{t(allowable)}$ = 0.90 × 307 = 276 psi (for the lift joints)

and in accordance wih paragraph 4-3*c*, the allowable tensile stress for the MCE load condition is:

$f_{t(allowable)}$ = 1.33 × 435 = 579 psi (for the parent concrete)

$f_{t(allowable)}$ = 1.33 × 307 = 408 psi (for the lift joints)

D-14. Critical Tensile Stresses for the Earthquake Load Cases

a. The critical tensile stresses are obtained by adding the dynamic response tensile stresses with the static stresses at the node points along the upstream and downstream faces of the dam. These tensile stresses are then compared to the allowable tensile stresses to determine the acceptability of the design.

b. The following tabulations show the critical tensile stresses for the MCE. Also shown in bold print are the locations where the critical tensile stress exceeds the allowable tensile stress along with the percent overstress for these locations.

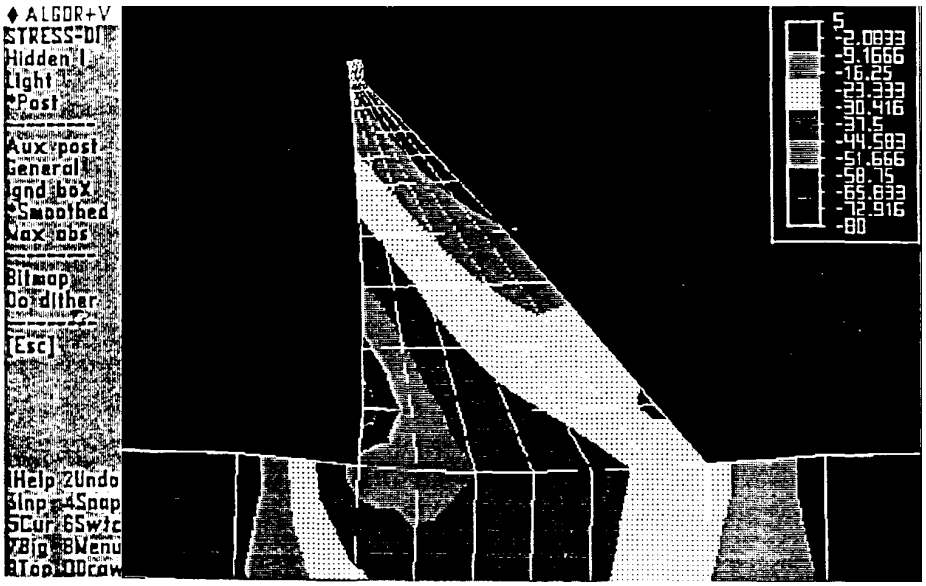

Static Stresses Normal to the Lift Joints (KSF, tension is +) - MCE Normal Pool Load Case

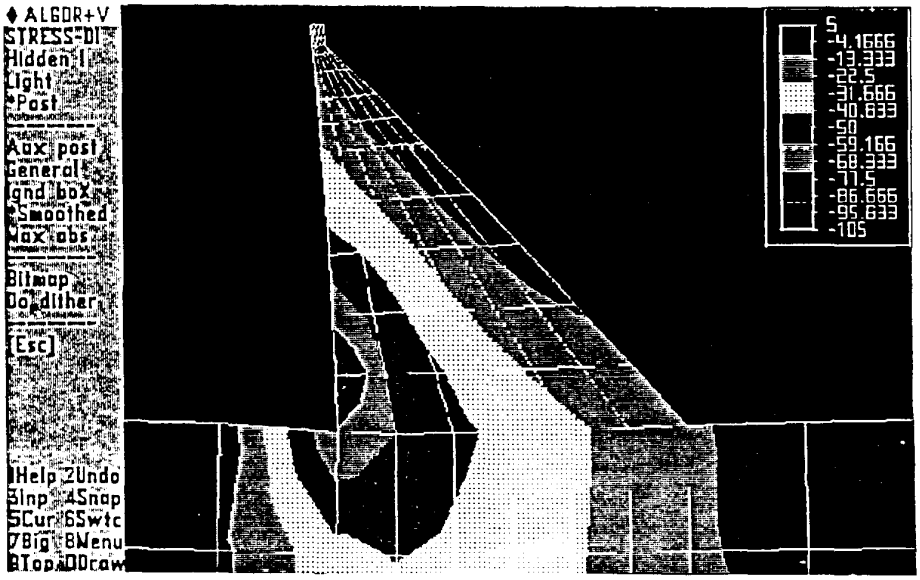

Static Stresses Normal to the Lift Joints (KSF, tension is +), - MCE Low Pool Load Case

Figure D-11. Static stresses normal to the lift joints - MCE load cases

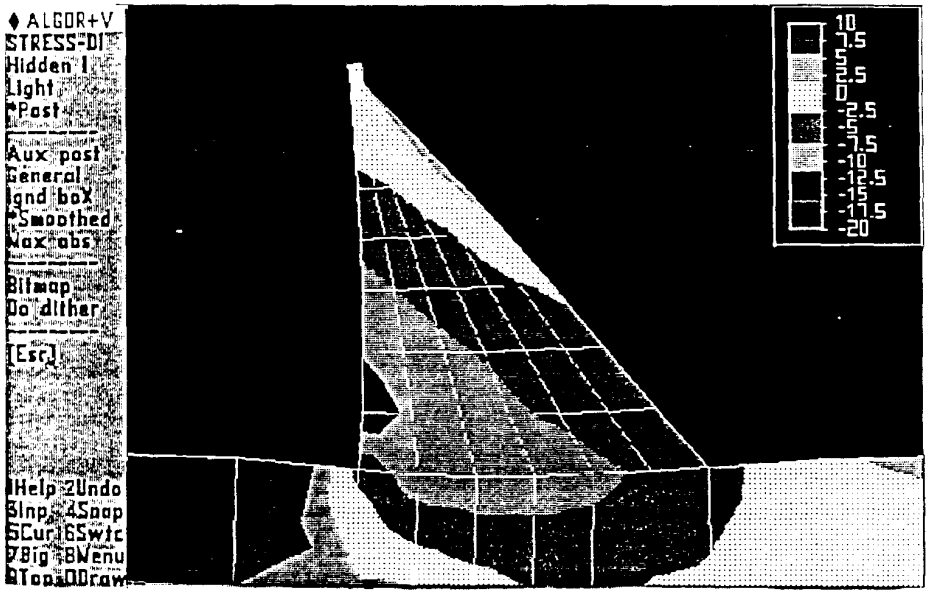

Principal Static Stresses (KSF, tension is +) - MCE Normal Pool Load Case

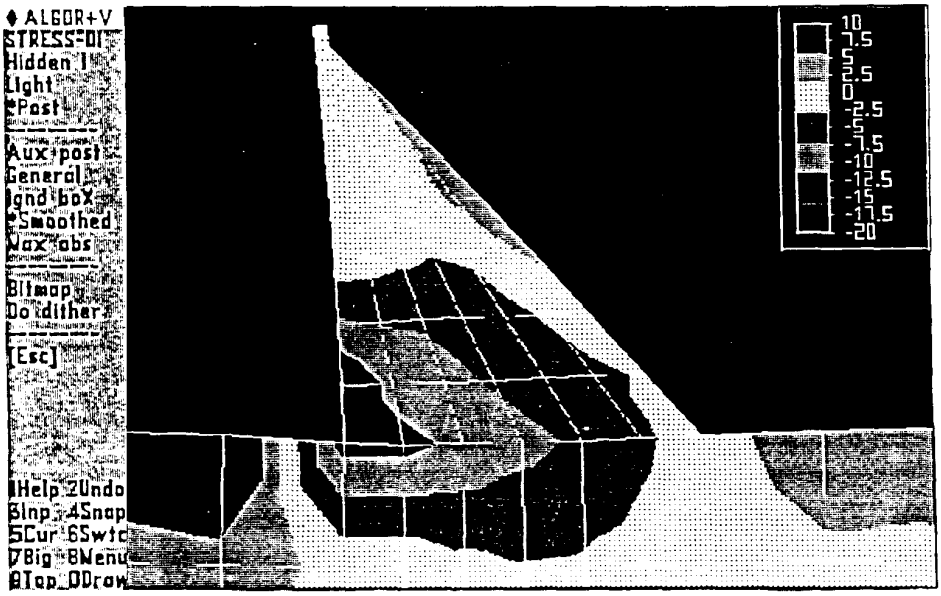

Principal Static Stresses (KSF, tension is +) - MCE Low Pool Load Case

Figure D-12. Principal static stresses - MCE load cases

MCE Normal Pool Load Case:
Critical Tensile Stresses Normal to the Lift Joints at the Upstream Face

Node No.	Stress Normal to the Lift Joint (ksf, tension is +)		Critical Tensile Stress (psi)	Percent Overstressed
	Dynamic Response	Static Stress		
143	12.52	-1.55	76	-----
129	53.23	-5.32	333	-----
115	57.06	-11.40	317	-----
108	65.15	-15.97	342	-----
101	76.27	-21.66	379	-----
94	84.29	-27.39	395	-----
87	95.30	-35.14	**418**	**2**
80	108.1	-45.25	**436**	**7**
73	122.2	-59.42	**436**	**7**
66	161.9	-78.37	**580**	**42**
56	113.8	-49.16	**449**	**10**

MCE Low Pool Load Case:
Critical Tensile Stresses Normal to the Lift Joints at the Upstream Face

Node No.	Stress Normal to the Lift Joint (ksf, tension is +)		Critical Tensile Stress (psi)	Percent Overstressed
	Dynamic Response	Static Stress		
143	13.35	-1.55	82	-----
129	56.84	-5.31	358	-----
115	59.98	-11.55	336	-----
108	68.03	-16.50	358	-----
101	80.83	-22.25	407	-----
94	88.26	-28.60	**414**	**1**
87	96.68	-37.15	**413**	**1**
80	106.8	-49.09	401	-----
73	118.3	-68.30	347	-----
66	154.8	-101.3	372	-----
56	108.3	-71.84	253	-----

MCE Normal Pool Load Case:
Critical Tensile Stresses Normal to the Lift Joints at the Downstream Face

Node No.	Stress Normal to the Lift Joint (ksf, tension is +)		Critical Tensile Stress (psi)	Percent Over-stressed
	Dynamic Response	Static Stress		
149	7.82	-1.53	44	-----
135	76.70	-2.77	**513**	**26**
121	39.77	0.16	277	-----
114	49.12	0.54	345	-----
107	59.55	0.19	**415**	**2**
100	67.83	-2.28	**455**	**12**
93	75.12	-8.04	**466**	**14**
86	79.57	-16.28	**440**	**8**
79	77.45	-25.06	364	-----
72	79.95	-33.68	321	-----
62	43.39	-24.10	134	-----

MCE Low Pool Load Case:
Critical Tensile Stresses Normal to the Lift Joints at the Downstream Face

Node No.	Stress Normal to the Lift Joint (ksf, tension is +)		Critical Tensile Stress (psi)	Percent Over-stressed
	Dynamic Response	Static Stress		
149	8.56	-1.53	49	-----
135	82.49	-2.72	**554**	**26**
121	42.66	-0.02	296	-----
114	51.86	0.06	361	-----
107	61.14	0.64	**429**	**5**
100	67.41	1.21	**477**	**17**
93	72.58	0.28	**506**	**24**
86	75.68	-3.44	**502**	**23**
79	73.05	-9.58	**441**	**8**
72	74.98	-15.40	**414**	**1**
62	40.63	-13.79	186	-----

MCE Normal Pool Load Case:
Critical Principal Tensile Stresses at the Downstream Face

Node No.	Principal Tensile Stress (ksf, tension is +)		Critical Tensile Stress (psi)	Percent Over-stressed
	Dynamic Response	Static Stress		
149	7.82	-1.53	44	-----
135	76.70	-2.77	513	-----
121	60.24	-1.75	406	-----
114	74.68	-2.09	504	-----
107	89.66	-2.90	**602**	**4**
100	103.7	-6.19	**677**	**17**
93	120.8	-13.69	**744**	**28**
86	126.0	-26.38	**692**	**20**
79	121.4	-40.07	564	-----
72	121.7	-52.48	481	-----
62	91.63	-46.83	311	-----

MCE Low Pool Load Case:
Critical Principal Tensile Stresses at the Downstream Face

Node No.	Principal Tensile Stress (ksf, tension is +)		Critical Tensile Stress (psi)	Percent Over-stressed
	Dynamic Response	Static Stress		
149	8.56	-1.53	49	-----
135	82.49	-2.72	554	-----
121	48.86	-1.84	326	-----
114	60.06	-1.70	405	-----
107	71.20	-1.36	485	-----
100	84.48	-1.89	574	-----
93	103.4	-4.51	**687**	**19**
86	112.2	-8.29	**722**	**25**
79	111.8	-14.80	**674**	**16**
72	113.5	-23.74	**623**	**8**
62	85.91	-24.10	429	-----

D-15. Conclusions and Recommendations

a. The critical tensile stresses shown in paragraph D-14*b* indicate certain areas or zones where superior RCC mixes are required so the RCC dam can be made to satisfy the earthquake resistant design criteria for new dams as established by this EP. Figure D-13 shows the zones that require RCC mixes with higher tensile capacity than the basic RCC mix with f'_c of 3,000 psi.

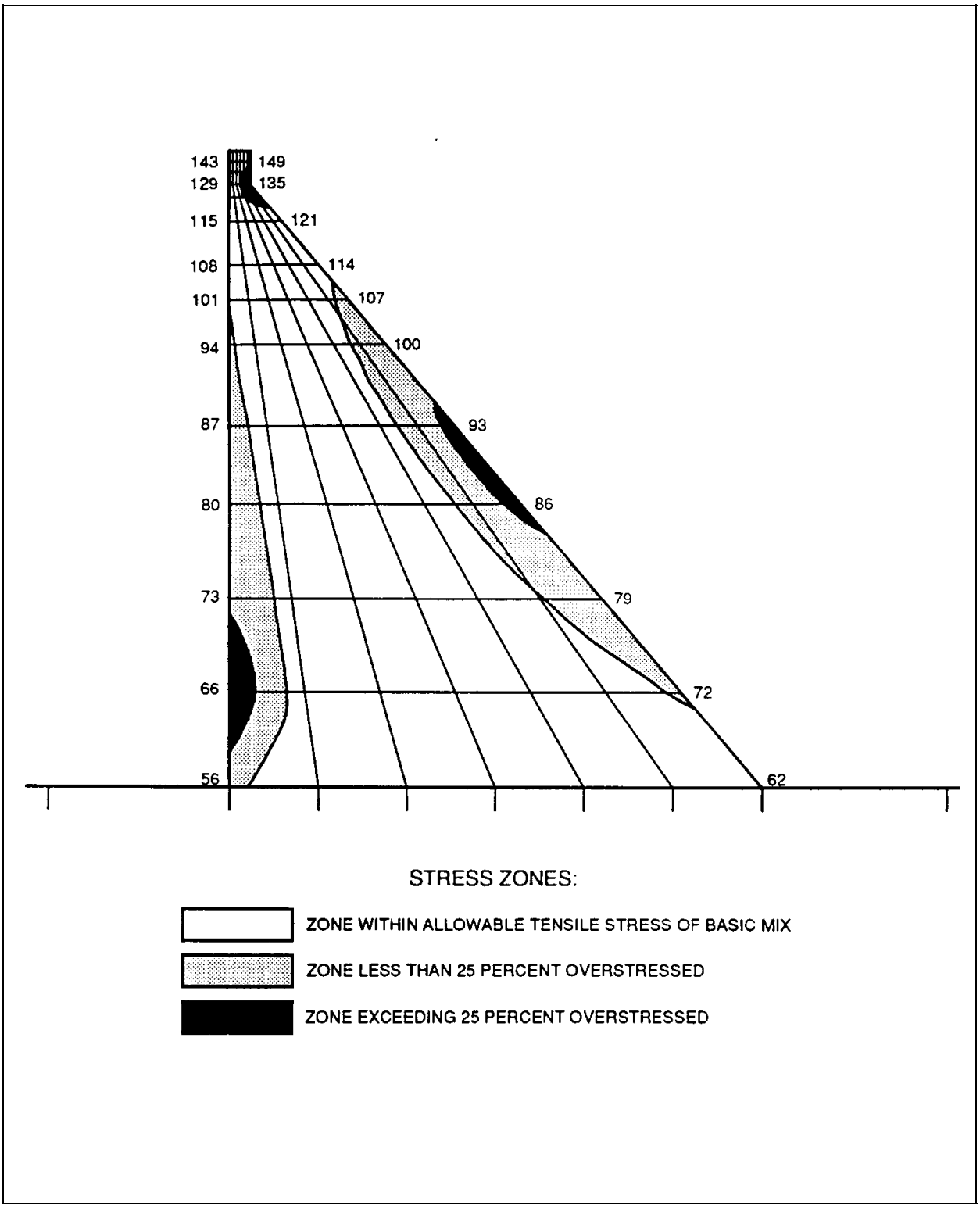

Figure D-13. Zones exceeding the allowable tensile stress for the basic RCC mix

b. The final step of the earthquake resistant design procedure would be to develop some higher strength RCC mix designs. Once the lab and field placement tests have been completed for these superior mixes, and their material properties established, the computer model shown in Figures D-1 and D-2 would be adjusted to reflect the zones of superior RCC. The dynamic analysis would be performed with the new computer model following the same procedure demonstrated above. If continued design upgrade attempts fail to meet the acceptability requirements, a more refined time-history analysis may be used to gain more insight regarding the dynamic response.

D-16. Comparing Response From Different Analysis Methods

a. Differences and similarities of attributes. In this appendix the design example problem was analyzed with the composite finite element-equivalent mass system method using a general purpose finite element program as discussed in paragraph 8-2*c*. In Appendix C, the same design example problem was analyzed using Chopra's simplified method as described in paragraph 8-2*a*. A comparison will now be made of the results produced by the two different methods of analysis. The earthquake loads for the normal reservoir condition will be used for the comparison. Referring to the attributes of dynamic analysis methods described in paragraph 8-1, the attribute differences and similarities for the two methods are:

(1) Material behavior - both methods used linear elastic material behavior. Material properties are identical for the two methods.

(2) Design earthquake definition - both methods used a design response spectrum to define the free field ground motion for the design earthquakes. Both methods anchored the design spectrum using the same PGA of 0.550 g.

(a) Differences in effective damping affect the response. The composite finite element method used a damping factor of 11.34 percent, and Chopra's method used a damping factor of 12.33 percent. Since damping in the response spectrum analysis is reflected in the spectral shape, the slightly higher damping in the Chopra analysis results in a slightly smaller response compared to the response produced by the composite finite element method.

(b) Another parameter associated with defining the design earthquake is whether both horizontal and vertical components of ground motion are specified or if only the horizontal component is specified. The composite finite element method used both horizontal and vertical components of ground motion. Chopra's simplified method is capable of only analyzing for the horizontal component of ground motion. As discussed in paragraph 7-8, the vertical component of ground motion can have significant effect on the response.

(3) Dimensional representation of project conditions - both methods used 2-D representation. The same 2-D cross section of the critical element of the dam was used in both analyses.

(4) Model configuration - the composite finite element method uses discrete finite elements to model the dam and a block of the foundation, and added mass to represent the hydrodynamic effects. Dynamic response is obtained by eigen solution of the stiffness and mass matrices. This type of equivalent mass system model is discussed in paragraph 8-1*d*(3). Chopra's simplified method uses a "standardized model" as discussed in paragraph 8-1*d*(1). With a "standardized model," dynamic loads are characterized by equivalent static load so that the stresses can be determined by either simple beam bending theory or by applying the equivalent static load to a finite element model of the dam fixed at the base. Appendix C utilized the latter method to determine the stresses because it provides a more realistic distribution of stress.

(a) Although the "standardized model" accounts for the foundation effects by increasing the fundamental period and the damping factor, its use of a simplified standard mode shape, based solely on horizontal translations relative to the fixed base, only approximates the 2-D deformations within the dam in response to the inertial effects of the ground motion. For example, the rigid body translation and rotational effect of the dam on its flexible foundation are not incorporated in the simplified approach. Therefore, the stress pattern produced by the two different analysis methods can be quite different at some locations in the dam.

(b) Another difference that can be considered as a part of the model configuration is the method used to combine the modal responses. In the composite finite element method the maximum modal responses

were combined by the Ten Percent Method (TPM) discussed in paragraph 7-7, where the modal responses for Chopra's simplified method were combined by square root of the sum of the squares method (SRSS). The TPM gives some additional accounting for modes of nearly the same frequency, and thus produces greater combined response.

b. Comparing common parameters. The following table compares the values of the parameters common to both methods of analysis:

Table of Common Parameters - MCE Normal Pool Load Case

Parameter	Chopra's Simplified Method	Composite Finite Element Method
T_1	0.443 sec	0.388 sec
R_r	1.100	1.075
R_w	0.85	1.00
R_f	1.190	1.336
$\tilde{T}_1$	0.585 sec	0.558 sec
β	12.33%	11.34%
$\tilde{S}_a$	22.37 ft/sec^2	22.26 ft/sec^2

c. Method for comparing results. To gain an understanding of the causes of the difference in the dynamic stress response as produced by the two analysis methods, several parameters will be adjusted to determine to what extent they contribute to the difference in stress response.

(1) The composite finite element analysis represents the more refined of the two analysis methods since its attributes and their associated parameters more closely represent the design conditions of the example problem. To determine how refinement of these parameters contributed to the difference in response, they will be set to the same value as was used in the simplified analysis. Adjustment of parameters is easy because of the flexible attribute capabilities of the composite finite element method as discussed in paragraph 8-2*c*(1).

(2) It is more difficult to adjust parameters in Chopra's simplified method because this method has primarily fixed attributes. However, one adjustment that is possible consists of placing the equivalent lateral static load on the same composite dam-foundation finite element model as was used in the more refined composite finite element analysis method. This will produce a more realistic stress pattern, particularly near the dam foundation interface because it allows for deformation of the foundation and associated redistribution of stresses from that of the fixed condition of the dam base as described in Appendix C.

(3) To help evaluate the difference in response of the two methods, a single parameter will be adjusted and an analysis made to determine it's effect on the stresses. A description of the adjustment of parameters follows. Note that Analysis #1 is the most refined analysis progressing sequentially to Analysis #6 which is the least refined analysis.

ANALYSIS #1: The composite finite element-equivalent mass system analysis as presented in this appendix with no modifications.

ANALYSIS #2: Analysis #1 modified by deleting the vertical component of ground motion.

ANALYSIS #3: Analysis #2 modified by using SRSS to combine the maximum modal responses.

ANALYSIS #4: Analysis #3 modified by using a 12.33 percent effective damping factor.

ANALYSIS #5: Chopra's simplified method as presented in Appendix C, but the stresses are determined by applying the equivalent static load on a composite finite element model of the dam-foundation as discussed above in paragraph D-16*c*(2).

ANALYSIS #6: Chopra's simplified method as presented in Appendix C with no modifications.

MCE Normal Pool Load Case:
Critical Tensile Stresses Normal to the Lift Joints at the Upstream Face

	Critical Tensile Stress (psi)					
	Composite Finite Element Method				Chopra's Method	
Node No.	Analysis #1	Analysis #2	Analysis #3	Analysis #4	Analysis #5	Analysis #6
143	76	72	71	68	196	196
129	333	315	313	302	262	262
115	317	293	291	279	198	198
108	342	312	310	297	186	187
101	379	343	341	326	205	205
94	395	354	353	336	206	204
87	**418**	371	370	351	210	205
80	**436**	385	385	363	218	224
73	**436**	385	385	360	219	281
66	**580**	**535**	**534**	**500**	316	**494**
56	**449**	**428**	**428**	404	285	247

MCE Normal Pool Load Case:
Critical Tensile Stresses Normal to the Lift Joints at the Downstream Face

	Critical Tensile Stress (psi)					
	Composite Finite Element Method				Chopra's Method	
Node No.	Analysis #1	Analysis #2	Analysis #3	Analysis #4	Analysis #5	Analysis #6
149	44	42	41	40	94	94
135	**513**	**493**	**490**	**474**	**527**	**527**
121	277	265	264	255	239	239
114	345	330	329	319	305	305
107	**415**	398	398	385	378	377
100	**455**	**440**	**439**	**425**	**422**	**418**
93	**466**	**453**	**453**	**437**	**430**	**427**
86	**440**	**431**	**431**	**414**	395	398
79	364	357	357	340	310	307
72	321	311	311	294	253	188
62	134	125	125	115	93	44

MCE Normal Pool Load Case:
Critical Principal Tensile Stresses at the Downstream Face

	Critical Tensile Stress (psi)					
	Composite Finite Element Method				Chopra's Method	
Node No.	Analysis #1	Analysis #2	Analysis #3	Analysis #4	Analysis #5	Analysis #6
149	44	42	41	40	98	98
135	**513**	**493**	**490**	**474**	**607**	**607**
121	406	455	453	374	395	396
114	504	482	482	466	493	493
107	**602**	579	579	560	**593**	**593**
100	**677**	**655**	**655**	**633**	**657**	**656**
93	**744**	**725**	**724**	**699**	**702**	**701**
86	**692**	**679**	**679**	**652**	**637**	**643**
79	564	554	554	527	493	498
72	481	463	463	437	385	305
62	311	290	290	270	234	67